Am J Cancer Res 2025;15(6):2807-2825
www.ajcr.us /ISSN:2156-6976/ajcr0164132

Original Article

ESRP1 drives subtype-specific breast cancer progression through ER-regulated transcriptional programs and EMT-related splicing switch

Xinyi Wang[1,2], Shuping Song[2], Weixuan Lin[5], Jiandi Huang[2,3], Wenchao Zhong[2,3], Donghang Li[2,3], Cainan Huo[2], Yongxuan Wang[5], Dingke Chen[1], Zhi Zhang[4], Yanqin Sun[1,2]

[1]Cancer Center, The Affiliated Dongguan Songshan Lake Central Hospital, Guangdong Medical University, Dongguan, Guangdong, The People's Republic of China; [2]Department of Pathology, School of Basic Medicine, Guangdong Medical University, Zhanjiang, Guangdong, The People's Republic of China; [3]Department of Pathology, The Affiliated Hospital of Guangdong Medical University, Zhanjiang, Guangdong, The People's Republic of China; [4]Department of Thyroid and Breast Surgery, Dongguan Songshan Lake Central Hospital, Guangdong Medical University, Dongguan, Guangdong, The People's Republic of China; [5]The First Clinical Medical College, Guangdong Medical University, Zhanjiang, Guangdong, The People's Republic of China

Received February 24, 2025; Accepted June 16, 2025; Epub June 25, 2025; Published June 30, 2025

Abstract: Epithelial Splicing Regulatory Protein 1 (ESRP1), an epithelial splicing regulator, influences the invasiveness and metastasis of breast cancer cells, yet its prognostic significance and interaction with estrogen receptors are not fully understood. Our findings indicate that ESRP1 is significantly up-regulated in breast cancer tissues and correlates positively with adverse clinical outcomes, particularly in estrogen receptor (ER) positive breast cancer. In vitro experiments with cells demonstrated a dual regulatory mechanism: in ER-positive breast cancer cells, reduced expression of ESRP1 suppresses tumor cell proliferation but does not significantly affect tumor cell invasion and migration; conversely, in ER-negative breast cancer cells, ESRP1 hinders tumor progression by regulating the alternative splicing of epithelial-mesenchymal transition (EMT)-related genes. To investigate whether the presence of ER is a decisive factor in ESRP1's role, we treated ER-positive breast cancer cells with an ER inhibitor to induce EMT, followed by the knockdown of ESRP1, which further promoted the EMT process and enhanced the cells' invasive and migratory abilities. This study demonstrates that ESRP1 is a potential breast cancer prognostic marker with subtype specificity and its value as a molecular target needs to be accurately assessed in the context of breast cancer subtypes, as ESRP1 function may be highly dependent on the ER background.

Keywords: ESRP1, ER, EMT, breast cancer, dual role

Introduction

Breast cancer, one of the most common cancers in women around the world, has overtaken lung cancer as the leading new cancer in women [1]. Despite a decline in overall mortality, it remains the second cause of cancer-related death in women [2]. Recurrence and metastasis of breast cancer remain major challenges in treatment, making it crucial to study the pathological mechanisms of breast cancer and its regulatory factors.

The estrogen receptor (ER) is a ligand-activated nuclear transcription factor that mediates most of the estrogen response and plays a key role in the development of breast cancer. Approximately 70-75% of breast cancer patients are ER positive (ER+) [3], making ER an important target for the treatment of this type of cancer [4]. ER promotes the proliferation and survival of breast cells by regulating gene expression, and its expression level is closely related to the prognosis of breast cancer patients [5]. In recent years, selective estrogen receptor modulators (SERMs) and aromatase inhibitors (AIs) have become the standard therapies for ER+ breast cancer, but the problem of drug resistance still needs to be urgently addressed [6]. Additionally, functional differences between dif-

https://doi.org/10.62347/OXPE5390

ferent subtypes of ER (ERα and ERβ) in breast cancer have provided new directions for therapeutic strategies [7, 8].

Epithelial Splicing Regulatory Protein 1 (ESRP1) is a critical RNA-binding protein that plays a pivotal role in the regulation of alternative splicing of epithelial-mesenchymal transition (EMT)-related genes. This process is associated with the invasive and metastatic potential of breast cancer cells. For instance, ESRP1 has been shown to modulate the splicing of CD44, thereby promoting its conversion from standard isoform (CD44s) to splicing variants (CD44v), a process that is closely associated with the migratory and invasive potential of tumor cells [7, 9]. Furthermore, ESRP1 expression levels correlate with prognosis in a wide range of cancers, and low expression of ESRP1 is often associated with increased tumor malignancy and metastatic potential [10-12].

The interaction between ER and ESRP1 has gradually gained attention in breast cancer, with ER affecting the proliferation, migration, and invasive ability of tumor cells by regulating the expression of ESRP1. For example, the activation of ER leads to upregulation of ESRP1 in luminal breast cancer with poor prognosis, which in turn affects tumor progression [13]. Therefore, an in-depth study of the role of ER-ESRP1 axis in breast cancer will not only help to elucidate the molecular mechanisms of breast cancer, but may also provide new targets for clinical treatment.

The aim of this study was to investigate the interaction between ER and ESRP1 and its biological significance in breast cancer. By analyzing the expression levels of ESRP1 in breast cancer tissue samples, we investigated the functional differences between ER-positive and ER-negative breast cancer cells, and used RNA sequencing to reveal the regulatory mechanism of ESRP1 in the epithelial-mesenchymal transition (EMT) process. Finally, the importance of the ER-ESRP1 axis in breast cancer development was further clarified by verifying the regulatory role of ER on ESRP1 transcriptional activity.

The scientific significance of this study lies in revealing the pro- and anti-tumorigenic roles of ESRP1 in breast cancer cells, enabling a better understanding of its role in the tumor microenvironment. This finding not only helps to elucidate the mechanisms regulating the invasiveness and metastatic ability of breast cancer cells, but also may provide new targets for clinical treatment. Particularly in ER-positive breast cancer, high expression of ESRP1 is associated with poor prognosis, suggesting its potential as a potential prognostic marker. Additionally, the results of the study will provide a basis for the development of targeted therapeutic strategies against ESRP1, offering a new direction for future research and treatment and promoting the development of early diagnosis and personalized treatment of breast cancer.

Materials and methods

Tissue microarray and immunohistochemistry (IHC)

Human breast cancer tissue microarrays (Shanghai Outdo BioTech Co. Ltd., Cat. #HBreD140Su03, #HBre-Duc090Sur-01) of 118 breast cancer tissue samples and 90 paracancerous normal tissue samples were used to evaluate ESRP1 expression in breast cancer and paracancerous normal tissues. Slides were dewaxed, rehydrated, and heated in sodium citrate buffer for antigen retrieval. Endogenous peroxidase and nonspecific staining were then blocked with an immunohistochemical assay kit (MXB biotechnology, China, Cat. No. KIT-9720) according to the instructions. Slides were then incubated with a 1:400 dilution of ESRP1 antibody (Proteintech, China, Cat. No. 21045-1-AP) overnight at 4°C, followed by incubation with biotinylated secondary antibody for 2 hours. Immunostaining was performed using DAB horseradish peroxidase chromogenic kit (MXB biotechnology, China, Cat. No. DAB-1031), and the results were analyzed under a microscope after hematoxylin staining. The expression level of ESRP1 was evaluated by the IHC score, which was derived by multiplying the proportion score by the intensity score, with a positivity score of “1” (0%-25%), “2” (26%-50%), “3” (50%-75%), or “4” (>75%). Staining intensity was scored as “0” (negative staining), “1” (weak staining), “2” (moderate staining), or “3” (strong staining). The percentage of positively stained area in the result of the total immunostaining score with a multiplier for staining intensity ranges from 0 to 12. A total score of 0-4 indicates no expression

or low protein expression, and a total score of ≥6 indicates high expression.

Cell culture and transfection

Human breast cancer cell lines MDA-MB-231 (Cat. #TCH-C453) and MCF7 (Cat. #TCH-C247) were purchased from Haixing Biosciences, Suzhou, Jiangsu, China. MDA-MB-231 cell line was cultured in Duchenne modified Eagle's medium (DMEM, Gibco, China, Cat. #C119605-00BT) containing 10% Fetal Bovine Serum (Standard Grade, Excell, Uruguay, Cat. #FSS-500) and 1% Penicillin/Streptomycin (Solarbio, China, Cat. #P1400). MCF-7 cells were cultured in specialized medium (Haixing Biosciences, China, Cat. #TCH-G247). All cells were cultured at 37°C in % CO_2.

Small-interfering RNA (siRNA) targeting ESRP1 was designed and synthesized by Suzhou GenePharma Biotechnology Co. Ltd. The sequences of siRNAs (si-ESRP1-#1/2/3/4) are described in Table S1. siRNA transfection was performed using GP-transfect-Mate transfection reagent (GenePharma, Cat. No. #G04009, China) according to the manufacturer's protocol. Untargeted siRNA (siNC) was used as a negative control. cell biology and biochemistry experiments were performed after 48 hours.

The pcDNA3.1 plasmid was used as a cloning vector for overexpression. 3 plasmids were used to overexpress ESRP1, ESR1 and ESRP1 promoter, respectively. The pcDNA3.1-ESRP1, pcDNA3.1-ESR1 and ESRP1-promoter-GPL4 plasmids were constructed by GenePharma Biotechnology Co. Ltd. for overexpression of ESRP1 and ESR1. Empty vector was used as a negative control. 48 hours after transfection, cell biology and biochemistry experiments were performed.

Reverse transcription quantitative real-time PCR (RT-qPCR)

Total RNA was extracted using TRIzol (Invitrogen, USA, Cat. No. #10296010CN) according to the manufacturer's instructions. Reverse transcription was performed using the High-Capacity cDNA Reverse Transcription Kit (Thermo Fisher Applied Biosystems™, USA, Cat. No. #4368814) to obtain cDNA, and the cDNA was used for quantitative real-time PCR. Quantitative real-time PCR was performed using the 2× RealStar Green Fast Mixture with ROX kit (GenStar, China, Cat. #A303) according to the manufacturer's instructions. RT-qPCR results were analyzed by the comparative Ct method (2-ΔΔCt) using GAPDH gene expression as an endogenous control. Primer sequences used in this study are provided in Table S2.

Western blotting analysis

Total proteins were extracted using RIPA lysis buffer (Solarbio, Cat. #R0010, China) supplemented with a mixture of phenylmethylsulfonyl fluoride, protease inhibitors, and phosphatase inhibitors, and separated on 7.5%, 10%, and 12.5% SDS-PAGE gels (Epizyme Biotech, China). After electrophoresis, the separated protein bands were transferred to polyvinylidene fluoride membranes (Millipore, Cat. #IPVH00010), which were closed in 5% skim milk for 2 h at room temperature. The membranes were then incubated with the primary antibodies against ESRP1 (Proteintech, China, Cat. #21045-1-AP), ER (Proteintech, China, Cat. #20698-1-AP), E-Cadherin (Cell Signaling Technology, Cat. #3195, USA), β-Cantenin (Cell Signaling Technology, Cat. #8480, USA), ZO-1 (Cell Signaling Technology, Cat. #8193, USA) and Vimentin (Cell Signaling Technology, Cat. #5741, USA) at a diluted ratio of 1:1000 and GAPDH (Proteintech, Cat. #10494-1-AP) at a dilution of 1:50,000 overnight at 4°C. After three washes, the membranes were incubated with 1:5000 horseradish peroxidase-conjugated secondary antibodies (Cell Signaling Technology, Cat. #7074 and Cat. #7076) for 2 hours at room temperature. Finally, the membranes were washed three times and visualized using an ECL kit (Thermo Fisher, Cat. 34580).

Colony formation assay and CCK-8 cell proliferation assay

About 1000 cells were inoculated into each well of a six-well plate and cultured at 37°C, 5% CO_2 incubator for 14 days. The culture medium was discarded and the cells were fixed with paraformaldehyde for 30 min and stained with 0.1% crystal violet for 30 min.

Cell proliferation was detected using Cell Counting Kit-8 (Dojindo, Japan, Cat. #CK04). Logarithmic growth phase breast cancer cells (6×10^3) were counted and inoculated in 96-well plates in a volume of 100 μl in five replicate

wells. After 24, 48, 72 and 96 h of inoculation, 10 μl of reagent was added and incubated for 3 h. The absorbance was then measured at 450 nm.

Cell cycle assays

To measure the cell cycle distribution, MDA-MB-231 cells and MCF7 cells were transfected with oe-ESRP1 and si-ESRP1, respectively, for 24 h before harvesting and fixed in 70% ice-cold ethanol overnight. Cells were then washed with PBS and cell cycle distribution was detected using a cell cycle detection kit (Elabscience, China, Cat. #E-CK-A352). Cell cycle distribution was analyzed by flow cytometry according to the manufacturer's guidelines.

Wound healing assay

Cell migration was measured using a culture insert (Ibidi, Cat. 80209). A cell suspension with a density of 7×10^5/mL (70 μL by volume) was added to each well of the culture insert. A cell-free gap of 500 μm was created by removing the culture insert after the appropriate cell attachment time (24 hours). Images were taken every 6 hours using an inverted phase contrast microscope. Percent wound closure in five randomly selected fields of view was calculated using NIH ImageJ software.

Transwell migration and invasion assay

Transwell assays were performed using Transwell plates (24 wells, 8 μm pore size (Corning, Cat. #3422)). For migration assays, 1×10^5 cells were harvested in 100 μl of serum-free medium and added to the upper chamber without Matrigel For invasion assays, Transwell membranes were pre-coated with 30 μl of a 1:8 dilution of Matrigel (BD, Cat. #356234) prior to the addition of the cell suspension. Next, 600 μl of 20% fetal bovine serum medium was placed into the bottom compartment of the chamber as a source of chemoattractant. After 24 hours of incubation, the cells were fixed and filtered through the insert by crystal violet. Migrating cells were photographed and counted by inverted microscope (magnification 100×).

RNA sequencing

Total RNA from MCF7 and MCF7-si-ESRP1 was freshly extracted using TRIzol reagent (Takara, Cat. #9108). The clean reads were then aligned to 9606 (NCBI Taxonomy ID) genome (version: GRCh38) using the Hisat2. Guangzhou GeneCloudBio. Co., Ltd. applied HTseq to calculate the counts of the genes. RPKM/FPKM (Reads/Fragments Per Kilobase Million Reads) was used to standardize the expression data. All data were analyzed according to the manufacturer's protocol. Differentially expressed genes were then identified by fold change. The thresholds for up- and down-regulated genes were set to a fold change greater than 2.

Public database and bioinformatics analysis

The correlation of ESRP1 with ESR1 in TCGA breast tissues was analyzed using GEPIA online tool (http://gepia.cancer-pku.cn/). Based on the Gene Ontology database (https://geneontology.org/), the differential genes obtained from transcriptomics sequencing analysis were annotated with GOs at three levels, BP, MF, and CC, respectively, to obtain all the GOs involved in the genes, and the significance level (*P*-Value) of each GO was calculated using Fisher's test to filter out the significant GOs enriched by differential genes. The differential genes screened by transcriptomics sequencing were subjected to Pathway annotation based on the Kyoto Encyclopedia of Genes and Genomes database (https://www.kegg.jp/) to obtain all Pathway Term involved in the differential genes, and Fisher's test was used to calculate the significance level (*P*-Value) of each GO, so as to filter out the significant GOs enriched by the differential genes. Fisher's test was used to calculate the significance level (*P*-Value) of the Pathway to screen out the significant Pathway Term enriched with differential genes.

Immunofluorescence

1×10^5 cells per well were inoculated into 24-well plates and after 24 hours of incubation, cells were fixed with 4% paraformaldehyde and permeabilized with 0.1% Triton X-100/PBS. Non-specific staining was blocked by incubation in 5% bovine serum albumin/PBS for 2 hours. Subsequently, cells were incubated overnight at 4°C with a mixture of anti-ESRP1 antibody (Proteintech, China, Cat. #21045-1-AP) and anti-ER antibody (Servicebio, China, Cat. #GB121843-50) at a dilution of 1:100 overnight at 4°C, and then incubated in fluores-

Table 1. Expression of ESRP1 in cancer and paracancerous tissue tissues

Histological type	Total	ESRP1 expression		χ^2	p
		Low or negative (%)	High (%)		
Cancer tissue	118	43 (36.4)	75 (63.6)	29.6	0.0001
Paracancerous tissue	90	67 (74.4)	23 (25.6)		

cent-labeled secondary antibody at a dilution of 1:200 (Proteintech, Cat. # RGAM004, RGAR002) for 2 hours. Cell nuclei were stained with DAPI and images were captured by fluorescence inverted microscope at 100× and 400× magnification.

Dual luciferase assay

A total of 500 ng of GPL4 Basic plasmid (GenePharma, China, #C09005) and GPL4 plasmid inserted with the ESRP1 promoter sequence (TSS: -1899 ~ +100), as well as 1000 ng of empty and pcDNA3.1-ESR1 vector plasmid (GenePharma, China, #C05008) and 100 ng of Renilla luciferase pRL-TK plasmid (Promega, cat. #E2241) were cotransfected into HEK293T cells according to experimental groups. After 48 h, Dual-Luciferase assays were performed using a Dual-Luciferase reporter assay system (Promega, cat. #E1910) according to the manufacturer's protocol. Luciferase activity was measured as the ratio of the firefly luciferase signal to the Renilla luciferase signal. All measurements were standardized to the control group.

Statistical analysis

Data are expressed as mean ± standard deviation (SD) of at least three independent experiments. Data were analyzed primarily using the software GraphPad Prism 9.0 (Insightful Science, USA). Categorical variables (e.g., clinicopathological parameters) were compared using Pearson's chi-square test. For contingency tables with frequencies ≤5, Fisher's exact test was applied. Survival differences between groups were assessed by the log-rank test, with Kaplan-Meier curves visualizing time-to-event outcomes. Continuous variables (e.g., gene expression levels), were analyzed as follows: Comparisons of two independent groups used the unpaired Student's t-test (for normally distributed data) or Mann-Whitney U test (for non-normal distributions). Multi-group comparisons employed one-way ANOVA followed by Fisher's Least Significant Difference (LSD) post hoc test for selected pairwise comparisons when overall significance was detected. Longitudinal/repeated-measures data (e.g., cell viability at multiple timepoints) were evaluated using repeated-measures ANOVA. *P* values were considered statistically significant as follows: P<0.05 (*), P<0.01 (**), P<0.001 (***), and P<0.0001 (****).

Result

ESRP1 is relatively highly expressed in ER-positive breast cancer tissues and is positively associated with poor patient prognosis

To investigate the clinical significance of ESRP1 in breast cancer, we collected 118 breast cancer (BC) tissue samples and 90 paracancerous normal tissue samples and performed immunohistochemical staining (IHC) analysis. Based on the IHC score, cases with a score of ≥4 were defined as high ESRP1 expression, and cases with a score of <4 were defined as low or no expression. As shown in **Table 1**, in BC tissues, 75 cases (63.6%) showed high expression of ESRP1, and 43 cases (36.4%) showed low or negative expression. In contrast, in normal tissues adjacent to the cancer, only 23 cases (25.6%) showed high ESRP1 expression, and 67 cases (74.4%) showed low or negative expression. This indicated that the expression level of ESRP1 in BC tissues was significantly higher than that in normal tissues adjacent to cancer (*P*<0.001) (**Figure 1A**, **1B**).

Based on the complete clinical pathology data, this study screened out the patient cohort that met the inclusion criteria for statistical analysis by excluding cases with missing key indicators such as ER, PR, Her-2, and histological type, to ensure data integrity and the reliability of the results. Further analysis of the relationship between ESRP1 expression and clinicopathological characteristics of BC patients (**Table 2**) revealed that: ER-positive patients had significantly higher ESRP1 expression levels than ER-negative patients (*P*=0.0154) (**Figure 1C**). Additionally, high ESRP1 expression was significantly associated with lymph node meta-

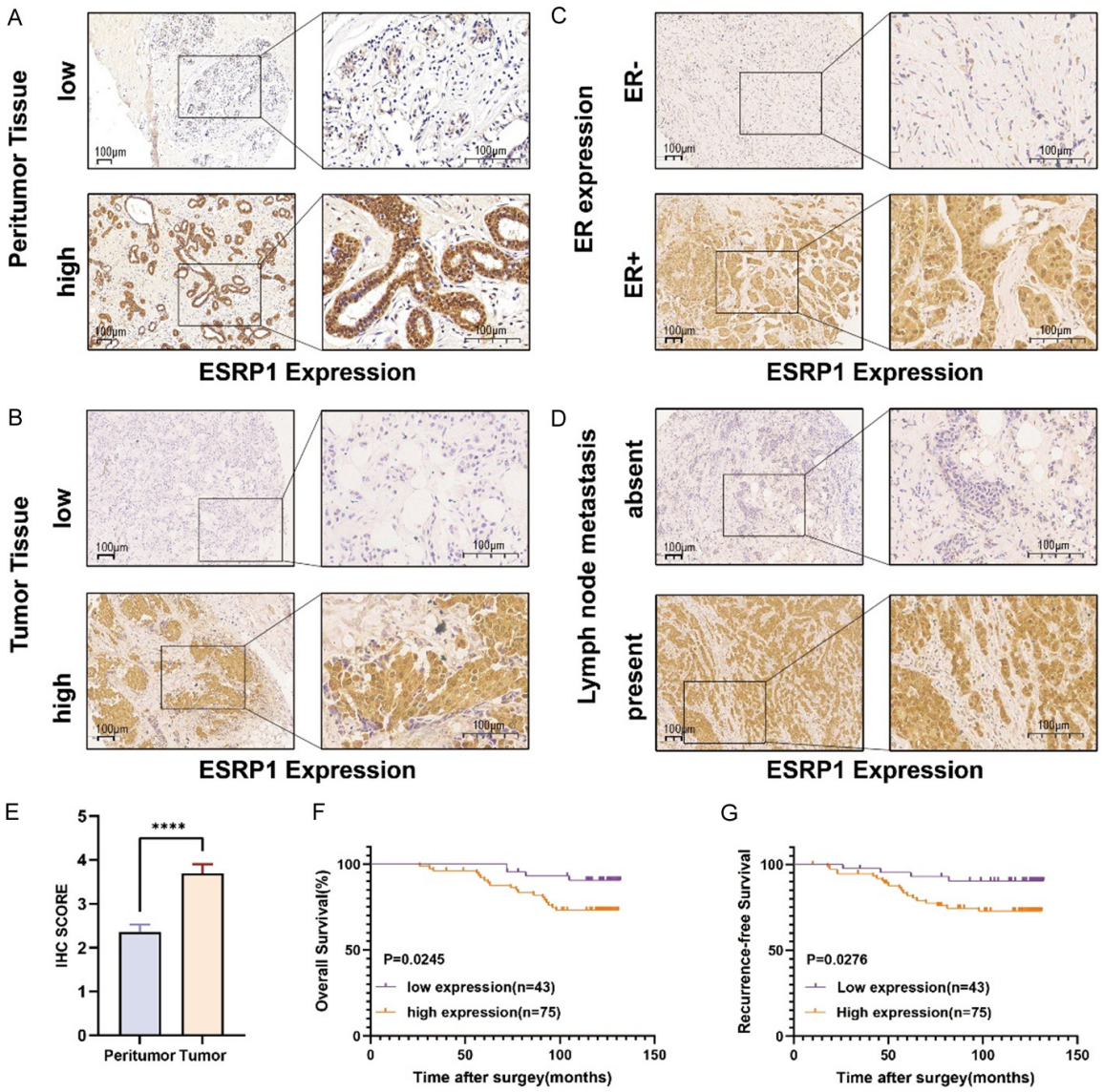

Figure 1. ESRP1 is relatively highly expressed in ER-positive breast cancer tissues and is positively associated with poor patient prognosis. A, B. Representative images of immunohistochemical staining of ESRP1 protein in normal and cancerous tissues adjacent to breast cancer, Scale bar: 100 μm, magnification, ×100, ×400. C, D. Representative immunohistochemical staining images demonstrating ESRP1 expression in tumors with different ER protein expression levels and the presence or absence of lymph node metastases. E. Immunohistochemical staining score (IHC score) of ESRP1 expression in 118 breast cancer and 90 peritumor specimens from breast cancer tissue microarrays. The expression level of ESRP1 in breast cancer tissues was significantly higher than that in normal tissues (****P<0.0001). F. Kaplan-Meier curves showing OS in patients with high ESRP1 expression versus negative or low ESRP1 expression. G. Kaplan-Meier curves showing RFS in patients with high ESRP1 expression versus ESRP1 negative or low expression.

stasis (P=0.0069) (**Figure 1D**). The IHC score of ESRP1 in tumor tissues was also significantly higher than that in peritumor tissues (P< 0.0001) (**Figure 1E**). In analyzing the expression of ESRP1 in different molecular types of BC, we found that there was no significant difference in the expression rate of ESRP1 in the clinical samples collected in this study. Of the 62 Luminal-type patients, 43 (69.4%) had high ESRP1 expression. Among the 13 Her-2+ patients, 7 (53.8%) had high ESRP1 expression, and among the 23 triple-negative breast cancer (TNBC) patients, 12 (52.2%) had high ESRP1 expression. There was no significant dif-

Table 2. Correlation between ESRP1 positive and clinicopathologic characteristics of breast cancer

Clinical characteristics	Total	ESRP1 expression		χ^2	*P*
		Low or negative (%)	High (%)		
Age					
≤50	43	16 (37.2)	27 (62.8)	0.017	0.8955
>50	75	27 (36.0)	48 (64.0)		
ER expression					
Low	38	20 (52.6)	18 (47.4)	5.867	**0.0154***
High	76	23 (30.3)	55 (69.7)		
PR expression					
Low	61	23 (37.7)	38 (62.3)	0.0497	0.8235
High	56	20 (35.7)	36 (64.3)		
Histological type					
Invasive ductal carcinoma	96	35 (36.5)	61 (63.5)	-	0.665[a]
Invasive lobular carcinoma	9	4 (44.4)	5 (55.6)		
Mucinous adenocarcinoma	8	4 (50.0)	4 (50.0)		
Grades					
II	82	32 (39.0)	50 (61.0)	-	0.229[a]
II-III	31	8 (25.8)	23 (74.2)		
III	5	3 (60.0)	2 (40.0)		
TNM stages					
TNMI	28	13 (46.4)	15 (53.6)	2.957	0.2280
TNMII	49	19 (38.8)	30 (61.2)		
TNMIII	41	11 (26.8)	30 (73.2)		
Lymph metastasis					
Absent	63	30 (47.6)	33 (52.4)	7.292	**0.0069***
Present	55	13 (23.6)	42 (76.4)		

**P*-values in bold are statistically significant. [a]Fisher's exact test.

ference in ESRP1 expression among Luminal, HER-2 overexpression and TNBC subtypes of breast cancer (*P*>0.05) (Table S3).

Kaplan-Meier survival analysis showed that patients with low or negative ESRP1 expression were superior to patients with high ESRP1 expression in terms of overall survival (OS, P=0.0245) (**Figure 1F**) and disease-free survival (DFS, P=0.0276) (**Figure 1G**). These results suggest that high ESRP1 expression may be positively associated with poor prognosis in BC patients, suggesting that ESRP1 may serve as a potential biomarker for breast cancer prognosis.

ESRP1 plays a dual regulatory role in the malignant phenotype of ER-positive and ER-negative breast cancer cells

To further investigate the association between high ESRP1 expression and shorter survival of BC patients, and the reason why the ESRP1 expression level in ER-positive patients was significantly higher than that in ER-negative patients, we selected the ER-positive cell line MCF7 and the ER-negative cell line MDA-MB-231 cells (TNBC cell line) for in vitro studies. By RT-qPCR and Western blot (WB) experiments, we found that ESRP1 was highly expressed in MCF7 cells and lowly expressed in MDA-MB-231 cells (**Figure 2A**). To further validate the function of ESRP1, we transfected MDA-MB-231 cells with pcDNA3.1-ESRP1 plasmid to overexpress ESRP1 (**Figure 2B**), and knocked down the endogenous ESRP1 expression in MCF7 cells using siRNA (**Figure 2C**), RT-qPCR and WB analysis confirmed the changes in ESRP1 expression.

Next, we evaluated the effects of altered ESRP1 expression on cell proliferation. CCK-8 analysis and colony formation assays showed that knockdown of ESRP1 significantly inhibited

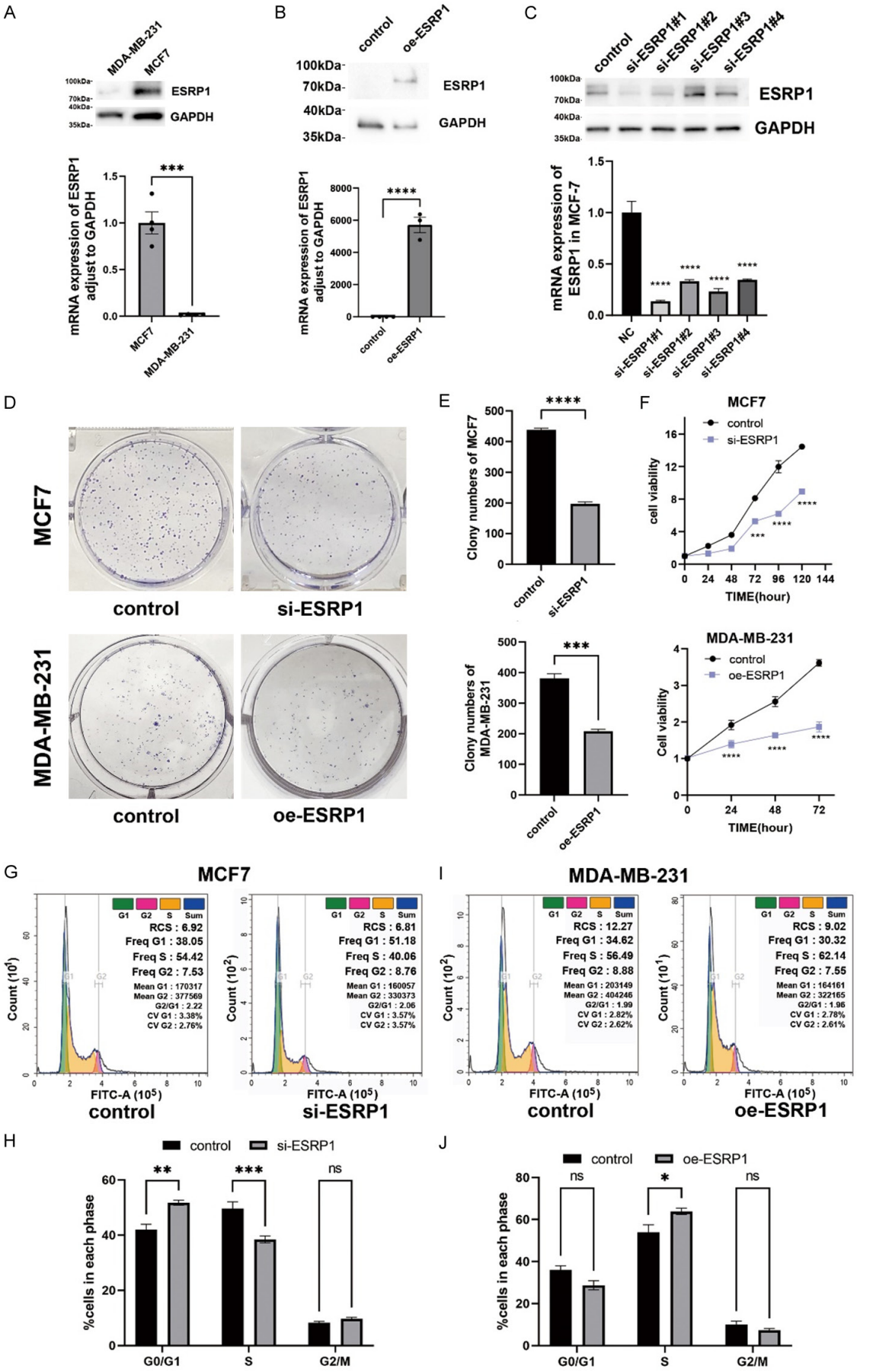
A
MDA-MB-231
MCF7
100kDa-
70kDa-
40kDa-
35kDa-
ESRP1
GAPDH
mRNA expression of ESRP1 adjust to GAPDH
***
MCF7
MDA-MB-231
B
control
oe-ESRP1
100kDa-
70kDa-
40kDa-
35kDa-
ESRP1
GAPDH
mRNA expression of ESRP1 adjust to GAPDH
****
control
oe-ESRP1
C
control
si-ESRP1#1
si-ESRP1#2
si-ESRP1#3
si-ESRP1#4
100kDa-
70kDa-
40kDa-
35kDa-
ESRP1
GAPDH
mRNA expression of ESRP1 in MCF-7
NC
si-ESRP1#1
si-ESRP1#2
si-ESRP1#3
si-ESRP1#4
D
MCF7
control
si-ESRP1
MDA-MB-231
control
oe-ESRP1
E
Clony numbers of MCF7
****
control
si-ESRP1
Clony numbers of MDA-MB-231
***
control
oe-ESRP1
F
MCF7
control
si-ESRP1
cell viability
TIME(hour)
MDA-MB-231
control
oe-ESRP1
Cell viability
TIME(hour)
G
MCF7
RCS : 6.92
Freq G1 : 38.05
Freq S : 54.42
Freq G2 : 7.53
Mean G1 : 170317
Mean G2 : 377569
G2/G1 : 2.22
CV G1 : 3.38%
CV G2 : 2.76%
control
RCS : 6.81
Freq G1 : 51.18
Freq S : 40.06
Freq G2 : 8.76
Mean G1 : 160057
Mean G2 : 330373
G2/G1 : 2.06
CV G1 : 3.57%
CV G2 : 3.57%
si-ESRP1
I
MDA-MB-231
RCS : 12.27
Freq G1 : 34.62
Freq S : 56.49
Freq G2 : 8.88
Mean G1 : 203149
Mean G2 : 404246
G2/G1 : 1.99
CV G1 : 2.82%
CV G2 : 2.62%
control
RCS : 9.02
Freq G1 : 30.32
Freq S : 62.14
Freq G2 : 7.55
Mean G1 : 164161
Mean G2 : 322165
G2/G1 : 1.96
CV G1 : 2.78%
CV G2 : 2.61%
oe-ESRP1
H
control
si-ESRP1
%cells in each phase
G0/G1
S
G2/M
J
control
oe-ESRP1
%cells in each phase
G0/G1
S
G2/M

Figure 2. ESRP1 plays a dual regulatory role in the malignant phenotype of ER-positive and ER-negative breast cancer cells. A. RT-qPCR as well as WB verified the difference in ESRP1 expression in MCF7 cells and MDA-MB-231 cells (***P<0.001). B. Western blot and RT-qPCR verified the overexpression of ESRP1 in MDA-MB-231 cells. control: empty vector; oe: overexpression (****P<0.0001). C. WB and RT-qPCR validated the knockdown of ESRP1 in MCF7 cells by a set of siRNAs; si-ESRP1#1 has a relatively high knockdown efficiency, so this siRNA was used in this study (***P<0.001, ****P<0.0001). D-F. The effects of knockdown of ESRP1 and overexpression of ESRP1 on the proliferative capacity of MCF7 and MDA-MB-231 cells were analyzed by clone formation assay and CCK-8 assay (***P<0.001, ****P<0.0001). G, H. Effect of ESRP1 knockdown on MCF7 cell cycle distribution, bar graphs showing the mean (± SD) of three experiments (**P<0.01, ***P<0.001). I, J. Effect of ESRP1 overexpression on the cell cycle distribution of MDA-MB-231, bar graph showing the mean (± SD) of three experiments (*P<0.05).

cell proliferation in MCF7 cells; whereas overexpression of ESRP1 also significantly inhibited cell proliferation in MDA-MB-231 cells (**Figure 2D-F**). This suggests that ESRP1 has differential effects on cell proliferation in different breast cancer cell lines: in ER-positive cells, ESRP1 promotes proliferation, while in ER-negative cells, ESRP1 inhibits proliferation.

To further explore the regulatory mechanism of ESRP1 on cell proliferation differences, we analyzed the effects of altered ESRP1 expression on cell cycle distribution using flow cytometry. In MCF7 cells, knockdown of ESRP1 resulted in an increased proportion of cells in the G0/G1 phase and a decreased proportion of cells in the S and G2/M phases (**Figure 2G**, **2H**), indicating that ESRP1 knockdown may inhibit cell proliferation by arresting the transition from the G0/G1 phase to the S phase. In contrast, in MDA-MB-231 cells, overexpression of ESRP1 resulted in a significant increase in the proportion of S-phase cells (**Figure 2I**, **2J**), suggesting that ESRP1 overexpression may inhibit cell proliferation by arresting the transition from the S-phase to the G2/M-phase. These results indicate that there are obvious differences in the regulatory effects of ESRP1 on the cell cycle in different breast cancer cell lines, which may be one of the reasons why ESRP1 plays a dual role in the proliferation phenotype of different breast cancer cells.

Loss of ESRP1 is known to induce EMT [14], we further investigated the effect of ESRP1 expression on the migration and invasion ability of breast cancer cells. Wound healing assay (**Figure 3A**, **3B**) and Transwell assays (**Figure 3C**, **3D**) showed that upregulation of ESRP1 significantly inhibited the migration and invasive ability of MDA-MB-231 cells, while ESRP1 expression had no significant effect on migration and invasion in MCF7 cells. To further explore the regulatory mechanism of ESRP1 in EMT, we detected the expression changes of key EMT-inducing transcription factors (EMT-TFs) and related proteins using WB. Knockdown of ESRP1 did not significantly alter the expression levels of the epithelial marker E-cadherin in MCF7 cells (**Figure 3E**, **3F**), as reported by Gökmen-polar et al. [15]. Suggesting that the oncogenic role of ESRP1 in ER-positive breast cancer may not be dependent on the EMT pathway. However, overexpression of ESRP1 significantly up-regulated the expression of E-cadherin in MDA-MB-231 cells, while down-regulating the expression of the mesenchymal marker Vimentin (**Figure 3G**, **3H**). Additionally, the mRNA levels of other EMT-associated transcription factors (SNAIL1 and SLUG) were significantly reduced (**Figure 3I**). It is suggested that ESRP1 may suppress tumor proliferation, invasion, and migration in TNBC by inhibiting EMT-related signaling pathways.

To further clarify the regulatory mechanism of ESRP1 in breast cancer progression, we performed RNA sequencing analysis on MCF7 cells with ESRP1 knockdown. The results showed that a total of 750 genes were significantly downregulated and 265 genes were significantly upregulated (**Figure 3J**). Through gene function enrichment analysis, we found that the downregulated genes were mainly enriched in the extracellular matrix (ECM) receptor signaling pathway (**Figure 3L**). Using the DAVID functional annotation tool, we further analyzed the biological processes that were significantly altered upon ESRP1 knockdown. The most notable functional clusters were cell adhesion-related genes (THBS1, THBS3, COL4A5, COL4A6, CD44, PKP1, PCDH1, and ITGB6) (**Figure 3K**). Although ESRP1 knockdown resulted in a significant down-regulation of the expression of cell adhesion-related genes, the migratory and invasive abilities of MCF7 cells were not significantly affected. The above suggests that in ER-positive breast cancer cells,

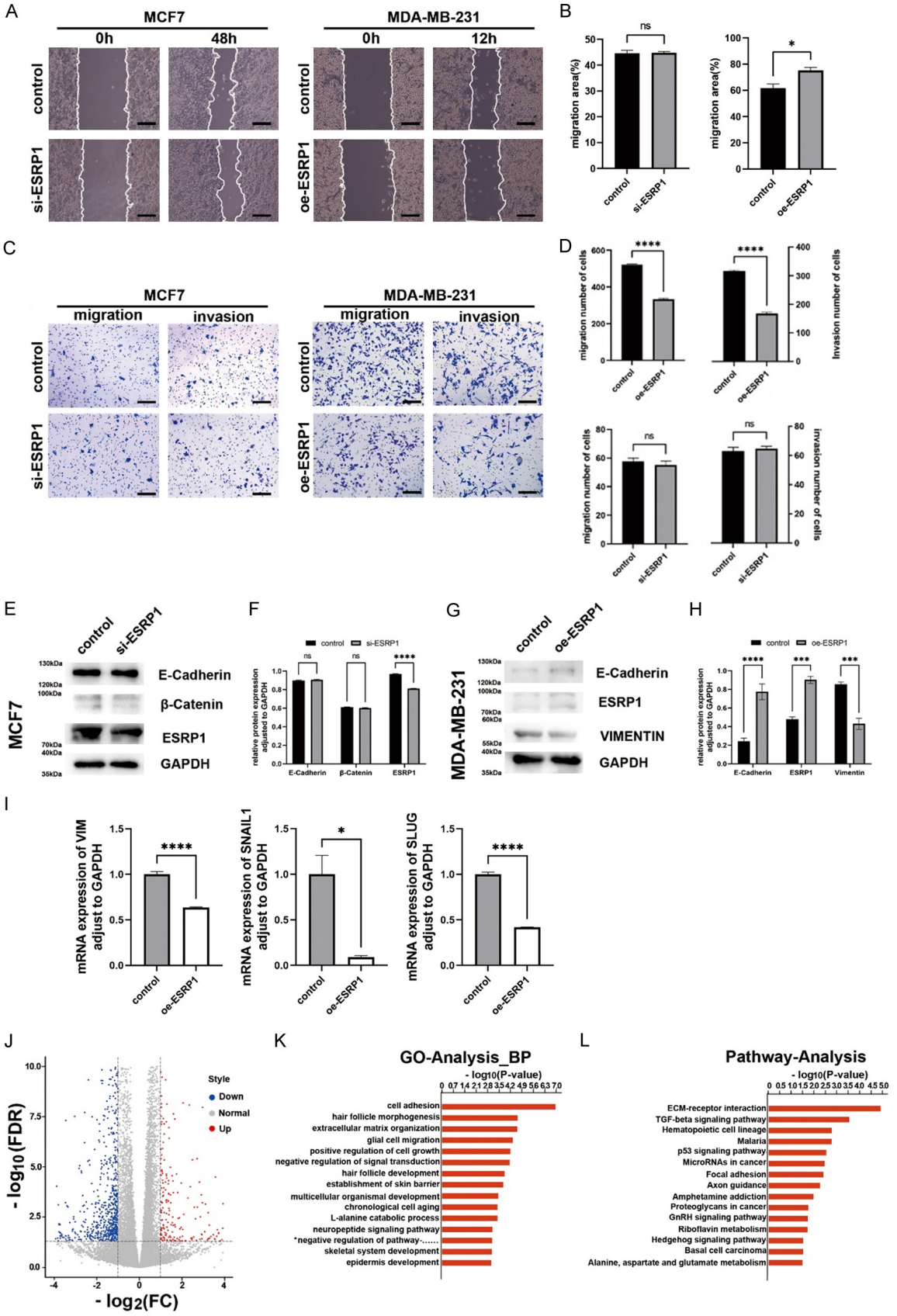
A
MCF7
0h
48h
MDA-MB-231
0h
12h
control
si-ESRP1
oe-ESRP1
B
ns
*
migration area(%)
control
si-ESRP1
oe-ESRP1
C
MCF7
migration
invasion
MDA-MB-231
D
****
ns
migration number of cells
invasion number of cells
E
control
si-ESRP1
MCF7
E-Cadherin
β-Catenin
ESRP1
GAPDH
F
relative protein expression adjusted to GAPDH
E-Cadherin
β-Catenin
ESRP1
G
oe-ESRP1
MDA-MB-231
E-Cadherin
ESRP1
VIMENTIN
GAPDH
H
***
Vimentin
I
mRNA expression of VIM adjust to GAPDH
mRNA expression of SNAIL1 adjust to GAPDH
mRNA expression of SLUG adjust to GAPDH
J
Style
Down
Normal
Up
- log10(FDR)
- log2(FC)
K
GO-Analysis_BP
- log10(P-value)
cell adhesion
hair follicle morphogenesis
extracellular matrix organization
glial cell migration
positive regulation of cell growth
negative regulation of signal transduction
hair follicle development
establishment of skin barrier
multicellular organismal development
chronological cell aging
L-alanine catabolic process
neuropeptide signaling pathway
*negative regulation of pathway-.....
skeletal system development
epidermis development
L
Pathway-Analysis
- log10(P-value)
ECM-receptor interaction
TGF-beta signaling pathway
Hematopoietic cell lineage
Malaria
p53 signaling pathway
MicroRNAs in cancer
Focal adhesion
Axon guidance
Amphetamine addiction
Proteoglycans in cancer
GnRH signaling pathway
Riboflavin metabolism
Hedgehog signaling pathway
Basal cell carcinoma
Alanine, aspartate and glutamate metabolism

Figure 3. Effect of ESRP1 on the migratory invasive effects of different subtypes of breast cancer cell lines. A, B. The effects of knockdown of ESRP1 and overexpression of ESRP1 on the migration ability of MCF7 cells and MDA-MB-231 cells were analyzed by scratch healing assay. Scale bar: 200 μm, magnification, ×200 (**P*<0.05). C, D. The effects of knockdown of ESRP1 and overexpression of ESRP1 on the migratory invasion ability of MCF7 cells and MDA-MB-231 cells were analyzed by Transwell assay. Scale bar: 200 μm (*****P*<0.05). E-H. Protein expression changes of key EMT-TFs in MCF7 cells and MDA-MB-231 cells after knockdown of ESRP1 and overexpression of ESRP1 were compared using Western blot as well as quantitative analysis of relative gray values (****P*<0.001, *****P*<0.0001). I. RT-qPCR verified changes in mRNA expression of key EMT-TFs in MDA-MB-231 cells after overexpression of ESRP1 (**P*<0.05, *****P*<0.0001). J. Volcano plot showing the distribution of significant gene expression changes in MCF7 cells after knockdown of ESRP1. K. Results of GO analysis of the biological process of down-regulation of differential genes in MCF7 cells after knockdown of ESRP1 (The full name of term marked with an asterisk is negative regulation of pathway-restricted SMAD protein phosphorylation). L. Results of KEGG signaling pathway analysis of down-regulated differential genes in MCF7 cells after knockdown of ESRP1.

although ESRP1 knockdown altered some of the biological processes, these changes may not be sufficient to significantly affect the morphological EMT and migratory/invasive functions of the cells. These results suggest that ESRP1's role in EMT in breast cancer may require specific background conditions, such as deletion of ER expression or synergistic effects of other signaling pathways.

ER promotes ESRP1 expression through transcriptional levels

Combined with the above results, ESRP1 plays different regulatory roles in the malignant phenotype of BC cells, which is significantly dependent on ER expression. Therefore, we further explored whether ER plays a regulatory role in ESRP1 through direct targeting binding or indirect regulation. Immunofluorescence experiments showed that ER and ESRP1 were mainly co-localized outside the nucleus in MCF7 cells (**Figure 4A**). According to the GEPIA database, the ESR1 gene (the gene encoding the ER protein) was moderately correlated with the ESRP1 gene in TCGA breast tissues (R=0.5, P=2.6e-08) (**Figure 4D**). It has been demonstrated that unliganded estrogen receptor alpha (apoERα), can undergo chromatin interactions independently of estrogenic stimulation [16, 17]. To verify the regulatory effect of ER on ESRP1, we degraded ER in MCF7 cells using the selective estrogen receptor degrader (SERD). Immunestrant, and detected the changes in ESRP1 expression after ER degradation using WB and RT-qPCR. The results showed that both mRNA and protein expression levels of ESRP1 were significantly down-regulated after ER degradation (**Figure 4B**, **4C**). After 14 days of continuous administration, ER protein expression was down-regulated by about 75-80%, further confirming the positive regulatory effect of ER on ESRP1.

To further validate this regulatory mechanism, we overexpressed ER (ESR1) in MDA-MB-231 cells and detected changes in ESRP1 expression using RT-qPCR. The results showed that the expression of ESRP1 was significantly elevated 4 days post-transfection compared to 2 days post-transfection (**Figure 4E**, **4F**). By analyzing the ESRP1 promoter region, we identified multiple ER binding sites upstream of it (**Figure 4G**), suggesting that ER may regulate the transcription of ESRP1 promoter region by directly binding to it. To test this hypothesis, we performed dual luciferase reporter system experiments, which showed that the fluorescence intensity was significantly higher after co-transfection of ER with the ESRP1 promoter than the control group transfected with the ESRP1 promoter alone (**Figure 4H**). These results suggest that ER can specifically bind to the ESRP1 promoter region and enhance its transcriptional activity.

Role of the ER-ESRP1 regulatory axis in breast cancer cell migration and invasion

Previous results showed that knockdown of ESRP1 in ER-positive breast cancer cells did not induce EMT development and did not affect cell migration and invasion phenotypes. If knockdown of ESRP1 after degrading ER in the cells by intervention could induce EMT development? Based on this consideration, we performed morphological and functional analyses of MCF7 cells treated with the SERD, Immunestrant. Compared with the DMSO control group, MCF7 cells underwent significant epithelial-mesenchymal transition (EMT) after 14 days of continuous administration, as evidenced by a change in cell morphology from a

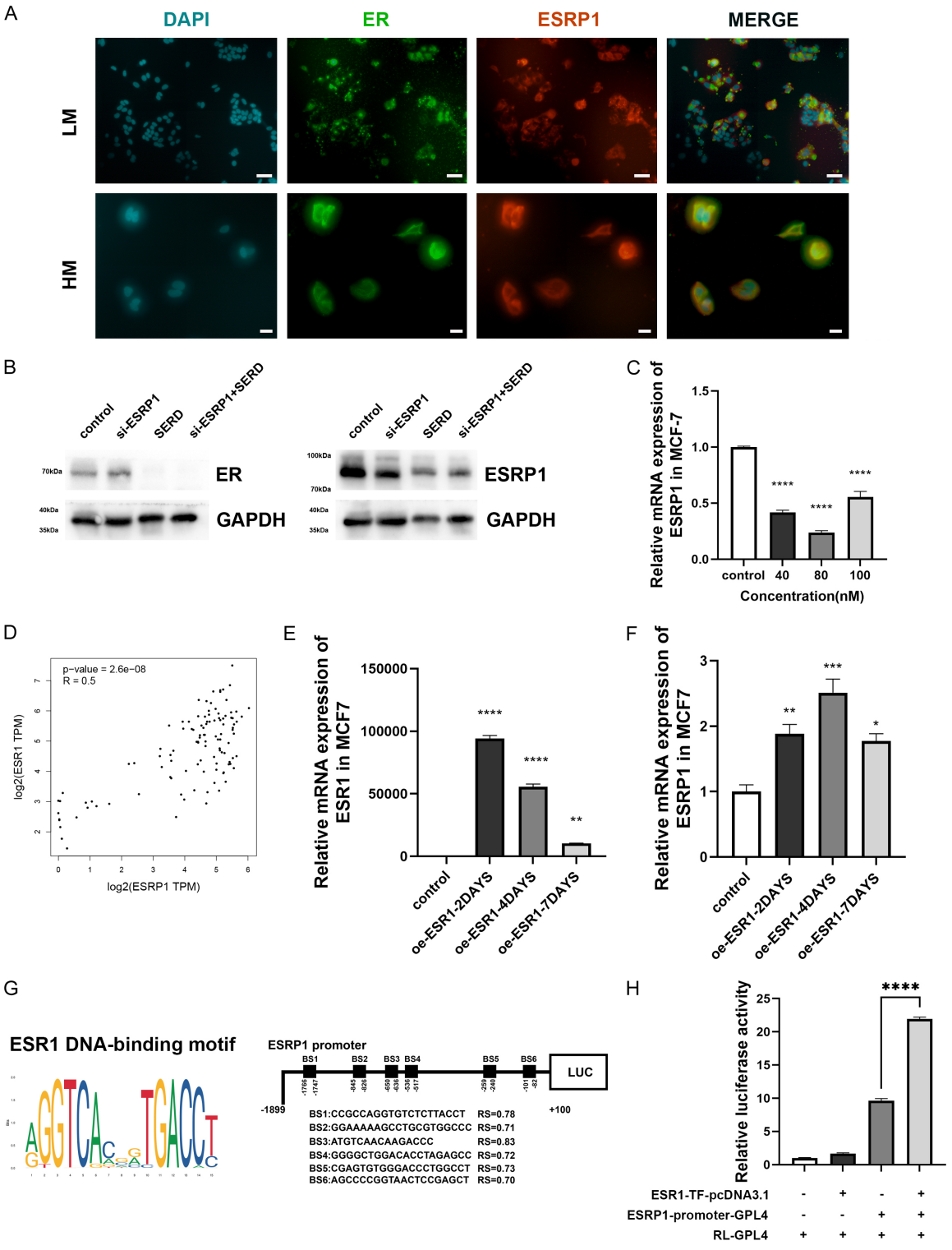

Figure 4. ER promotes ESRP1 expression through transcriptional levels. A. Immunofluorescence staining was performed to observe the localization of ER and ESRP1 in MCF-7 cells. Low magnification scale bar: 100 μm, high magnification scale bar: 20 μm, magnification, ×200, ×400. B. Comparison of ER and ESRP1 protein expression changes in MCF7 cells after use of selective estrogen receptor degraders (SERD) using WB. C. mRNA expression analysis of ESRP1 after degradation of ER using different concentrations of SERD (****P<0.0001). D. Correlation of ESR1 gene with ESRP1 gene in TCGA breast tissue was analyzed using GEPIA database (R=0.5, P=2.6e-08). E, F. RT-qPCR was used to verify the overexpression of ESR1 and to analyze the changes in mRNA expression of ESRP1 after overexpression of ESR1 in MDA-MB-231 cells (*P<0.05, **P<0.01, ****P<0.0001). G. DNA binding motifs of

the ESR1 gene (left) Schematic showing the ESRP1 promoter (-1899 to +100 bp) construct for luciferase reporter gene assay. Prediction of possible binding sites for ESR1 on the ESRP1 promoter by the JASPAR database. H. Relative fluorescence intensity changes were analyzed using a dual luciferase reporting system (****P<0.0001).

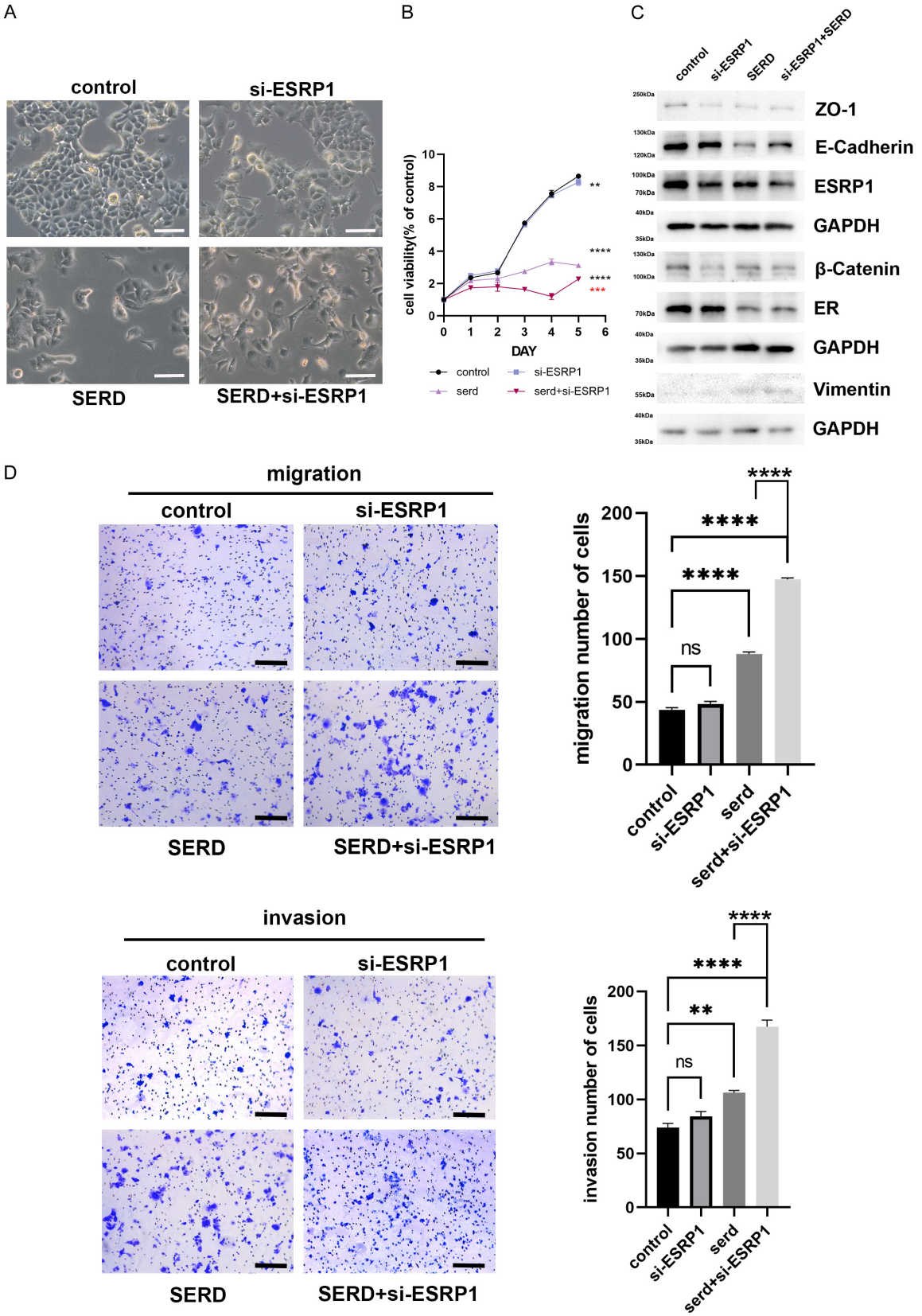

Figure 5. Role of the ER-ESRP1 regulatory axis in breast cancer cell migration and invasion. A. Representative images of MCF7 cells after knockdown of ESRP1 alone with SERD alone and after combined use of SERD and knockdown of ESRP1. Scale bar: 100 μm, magnification, ×400. B. The effects of si-ESRP1, SERD and si-ESRP1+SERD on the proliferative capacity of MCF7 cells were analyzed by CCK-8 assays. ***P*<0.01, ***P<0.001 (The *P* value in black represents compared with the control group, and the *P* value in red represents compared with the SERD group). C. Protein expression changes of key EMT-TFs in MCF7 cells after knockdown of ESRP1 alone versus SERD degraders alone and combination of SERD degraders and knockdown of ESRP1 were compared using WB. D. The effects of knocking down ESRP1 alone with SERD degraders alone and the combination of SERD degraders and knocking down ESRP1 on the migratory invasive ability of MCF7 cells were analyzed by Transwell assay. Scale bar: 200 μm, magnification, ×200. ***P*<0.01, *****P*<0.0001.

typical epithelial-like to a spindle-like mesenchymal form. The cells no longer grew in tightly packed colonies but appeared dispersed (**Figure 5A**), suggesting decreased cell-cell junctions and adhesion, indicating that ER deficiency induces EMT in breast cancer cells. Additionally, after SERD treatment, cell proliferation ability was significantly inhibited (**Figure 5B**).

To further investigate the role of ESRP1 under ER-deficient conditions, we knocked down ESRP1 in SERD-treated MCF7 cells. The results showed that the mesenchymal morphology of the cells was more pronounced after knocking down ESRP1, suggesting that ER deficiency and ESRP1 knockdown synergistically promote the EMT process. WB analysis of EMT-related markers revealed that in the SERD-treated group, the expression of epithelial markers E-cadherin and β-catenin was significantly reduced, while the expression of the mesenchymal marker Vimentin was significantly elevated. These changes were more pronounced under the condition of SERD combined with ESRP1 knockdown (**Figure 5C**).

Transwell assay further confirmed that combination of SERD and ESRP1 knockdown significantly enhanced the invasive and migratory abilities of MCF7 cells (**Figure 5D**). The above results suggest that loss of ER can induce EMT in breast cancer cells, and further knockdown of ESRP1 expression can further promote the EMT process.

Additionally, RT-qPCR results showed that the expression of EMT-associated transcription factors SNAIL1 and SLUG was significantly upregulated after ER degradation. We also validated previous transcriptome sequencing results and found that the expression of extracellular matrix (ECM) signaling pathway-related genes (THBS1, CD44, COL4A5, and TIMP1) was significantly downregulated (**Figure 6**). These results suggest that ER degradation and ESRP1 knockdown synergistically promote the EMT process in breast cancer cells and enhance their invasion and migration.

Discussion

ESRP1, an epithelial cell-specific RNA splicing factor, exhibits complex and context-dependent dual roles in multiple cancers. On one hand, ESRP1 inhibits tumor cell invasion and metastasis by regulating alternative splicing of EMT-related genes, which is associated with a favorable prognosis. For example, in lung cancer [18] and pancreatic cancer [19], the high expression of ESRP1 is closely associated with tumor suppressor function. It maintains the epithelial phenotype and inhibits the EMT process by regulating the splicing of genes such as CD44 and FGFR2. On the other hand, in breast and ovarian cancers, ESRP1 exhibits oncogenic effects [20-22]. In this study, we revealed the dual functions of ESRP1 and its regulatory mechanism in BC by analyzing clinical samples, in vitro functional experiments and molecular mechanism studies, providing a new theoretical basis for the precision treatment of breast cancer.

Our results showed that the expression level of ESRP1 in BC tissues was significantly higher than that in normal tissues adjacent to the cancer, and its high expression was closely associated with ER-positive status, lymph node metastasis and poor prognosis. This finding is consistent with the study of Gökmen-Polar et al. [15], who found that ESRP1 promotes tumor cell growth and drug resistance by regulating metabolic pathways (glycolysis and oxidative phosphorylation) in ER-positive breast cancer. However, Warzecha et al. reported that ESRP1 exerts tumor suppressive effects by inhibiting EMT in some breast cancer subtypes and is associated with a favorable patient prognosis

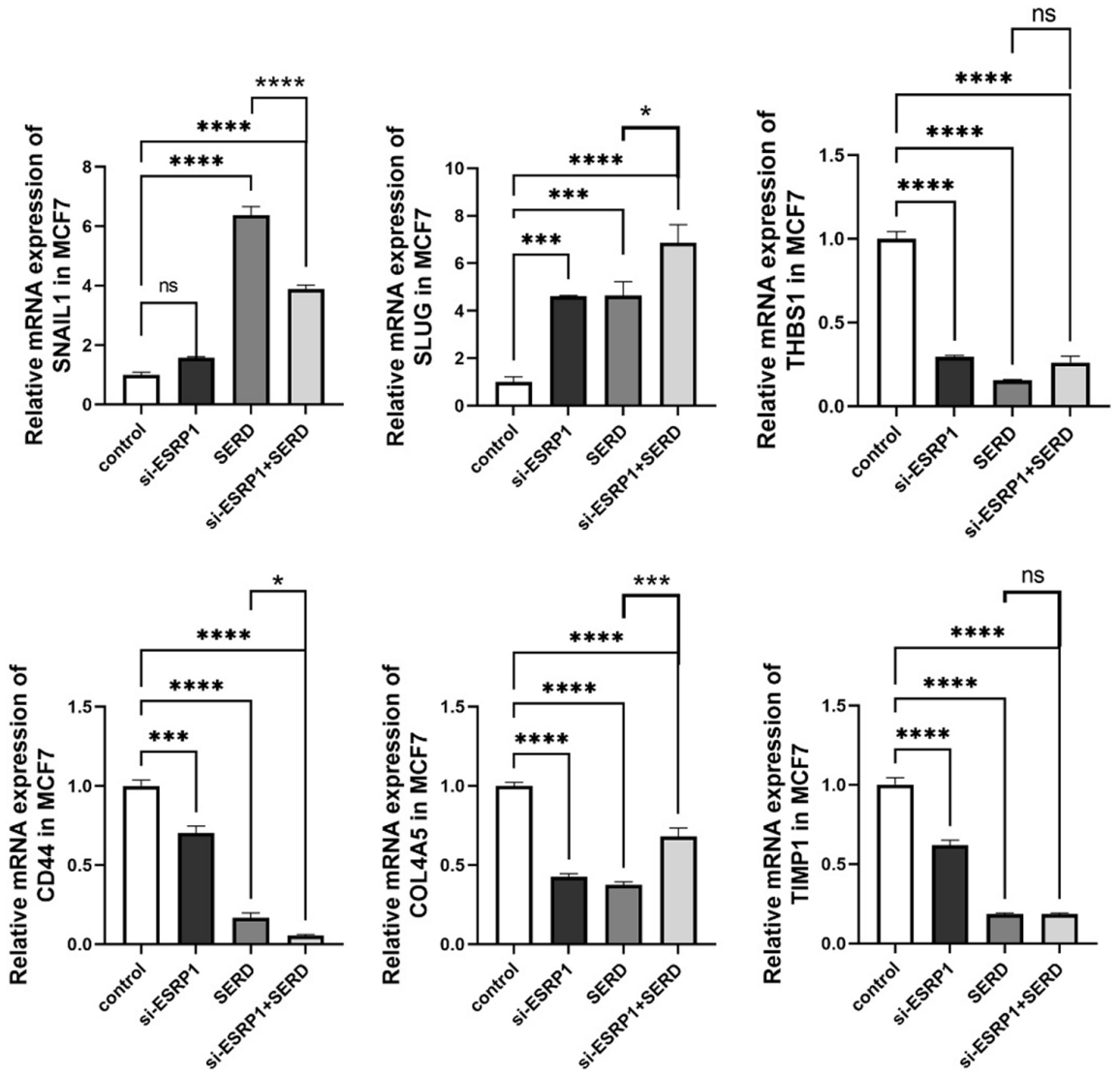

Figure 6. RT-qPCR validation of mRNA expression changes of key EMT-TFs and ECM signaling pathway-related genes in MCF7 cells (*P<0.5, ***P<0.001, ****P<0.0001).

[23-25]. Similarly, in our study, While ESRP1 expression was significantly higher in ER+ versus ER- tumors overall, the lack of difference across molecular subtypes (Luminal/Her-2+/TNBC) may reflect the complexity of subtype-specific biology. For instance, within the Luminal group, heterogeneity between Luminal A and Luminal B (potentially influenced by Her-2 or proliferation signals) could obscure subtype-level comparisons. Additionally, Her-2+ tumors, despite being ER-, may exhibit context-dependent ESRP1 suppression via Her-2/MAPK signaling. Her-2 and AXL form a heterodimer, activate the MAPK/ERK pathway, induce upregulation of EMT-related genes (e.g., ZEB1 and Vimentin), suppress the expression of the epithelial marker E-cadherin [26], and may also inhibit the expression of ESRP1, which is an epithelial phenotype-maintaining gene. GRHL2 and ESRP1 have both been identified as key regulators of EMT in TNBC [27], and there is functional complementarity and synergistic interaction between them; the GRHL2/ZEB feedback loop may alleviate the loss effect of ESRP1. The above studies reflect the context-dependent nature of ESRP1 exerting its biological functions. Future studies with larger subtype-stratified cohorts and mechanistic dissection of competing pathways are warranted to resolve these dynamics.

This complex role of ESRP1 was similarly found in our study. Through in vitro experiments, we found that ESRP1 promoted the proliferation of ER-positive BC cells (MCF7) and inhibited the proliferation and invasion of ER-negative BC cells (MDA-MB-231), suggesting that ESRP1's function in BC may be influenced by the ER. ER may further affect the regulation of cell cycle and EMT by ESRP1, indicating that ESRP1 has subtype-specific functions in BC. It is suggested that the function of ESRP1 may depend on the molecular typing and microenvironmental context of BC. Based on these findings, ESRP1 is expected to be applied in the clinic and become a potential target for precision treatment of BC. For example, targeting ESRP1 in ER-positive breast cancer may enhance the efficacy of endocrine therapy by inhibiting the metabolic pathway, whereas up-regulation of ESRP1 in TNBC may reduce the metastasis of tumors by inhibiting the EMT process.

ER plays a central role in the development and progression of breast cancer. ER not only regulates gene transcription through classical genomic pathways, but also influences cell signaling pathways and EMT processes through non-genomic pathways [19, 28]. Our study showed that ER regulates the transcriptional activity of ESRP1 promoter region by directly binding to it, thereby affecting the epithelial phenotype and invasive ability of BC cells. Additionally, the absence of ER led to the down-regulation of ESRP1 expression, which in turn promoted the EMT process in BC cells, as evidenced by the decreased expression of E-cadherin and elevated expression of Vimentin. This result is consistent with the study of Bouris et al. [29], suggesting that ER maintains the epithelial phenotype of BC cells and inhibits their invasion and metastasis through the regulation of ESRP1. However, the regulatory mechanism of ESRP1 may not be limited to ER. For instance, it has been shown that ESRP1 expression may be regulated by other transcription factors such as Twist and TGF-β [30, 31]. Therefore, future studies should further explore the regulatory network of ESRP1 in different signaling pathways.

The dual role of ESRP1 in breast cancer may be related to its regulation of EMT, a key process by which tumor cells acquire invasive and metastatic capabilities. In turn, key EMT-TFs in the EMT regulatory network have tissue environment specificity [32]. The role of ESRP1 in EMT regulation is likewise significantly context-dependent. Previous studies have shown that ESRP1 inhibits EMT in various tumors and low ESRP1 expression is associated with the development of EMT in ER-negative BC cells MDA-MB-231. However, our study found that knockdown of ESRP1 in ER-positive breast cancer MCF7 cells did not significantly alter the expression level of the epithelial marker E-cadherin, whereas EMT was induced by knockdown of ESRP1 after degradation of the ER receptor in MCF-7 cells. This is in line with the previous report by Gökmen-Polar et al. that in the absence of a proper context, ESRP1 splicing may not be sufficient to induce morphological EMT. ESRP1 splicing alone may not be sufficient to induce morphological EMT [15]. On the other hand, in MDA-MB-231 cells, ESRP1 overexpression significantly up-regulated the expression of E-cadherin, while down-regulated the expression of mesenchymal marker Vimentin, suggesting that ESRP1 may play an important role in the development of MDA-MB-231 cells, these results suggest that ESRP1 may inhibit EMT-related signaling pathways in TNBC. Cells undergo a loss of apical polarity, an increase in anterior-posterior polarity, a decrease in cell adhesion, a shift from an epithelial phenotype to a mesenchymal phenotype, and the acquisition of mesenchymal properties during the course of EMT. We further found through RNA sequencing that the most significantly altered biofunctional clusters after ESRP1 down-regulation in MCF7 cells were cell adhesion-related genes. It has also been reported that ESRP1-regulated ARHGEF11 isoforms necessary for the integrity of the splicing epithelial tight junction [33]. The weakening of intercellular adhesion was mainly in the early stages of EMT. EMT is a highly dynamic process that is regulated by multiple TFs. Some EMT-TFs (SNAIL, ZEB, and TWIST) can control the entire process, while others (FOXC1, FOXC2, and RUNX1) can only control part of the process [34]. Our results demonstrated that in ER-positive BC cells, ESRP1 knockdown was not sufficient to affect core transcription factor activity, and therefore no significant alterations were observed in the morphological characteristics of the cells and cell migration and invasion functions. In conclusion, the induction of EMT by ESRP1 in BC may require

specific contextual conditions, such as loss of ER expression or synergy of other signaling pathways.

Additionally, ECM remodeling plays an important role in the malignant progression of BC. ECM components such as collagen XII promote the invasion and metastasis of BC cells by regulating the mechanical properties of the tumor microenvironment [35]. According to our RNA sequencing analysis, ESRP1 knockdown resulted in a significant down-regulation of the expression of genes related to the ECM receptor signaling pathway, such as THBS1, COL4A5, and CD44, suggesting that ESRP1 may play an important role in the regulation of ECM signaling, It is suggested that ESRP1 may affect the malignant progression of BC by regulating ECM remodeling. Papanicolaou et al. [35] demonstrated a critical role of ECM components in BC metastasis. For example, THBS1 influences tumor invasion and metastasis by regulating cell adhesion and migration [36, 37]. However, although the expression of ECM-related genes was down-regulated by ESRP1 knockdown, the migration and invasion abilities of MCF7 cells were not significantly affected. The expression of ECM-related genes was more significantly down-regulated after further ER degradation, and ESRP1 knockdown significantly affected the migration and invasion ability of MCF7 cells in the context of ER degradation. This functional difference reflects the heterogeneity of the tumor microenvironment and the diversity of ESRP1 target genes, which may be related to the activity of the ER signaling pathway and the synergistic effect of other signaling pathways. Combined with the study of ESRP1 and ECM remodeling, future research could develop combined therapeutic strategies targeting the tumor microenvironment.

In conclusion, this study reveals the dual role of ESRP1 in BC and elucidates the molecular mechanism by which ER transcriptionally regulates ESRP1 expression. These findings provide new potential targets for precision treatment of BC. However, the functional mechanism of ESRP1 still needs further investigation, especially the functional differences in different BC subtypes and their relationship with treatment response. Future research should combine the regulation of the tumor microenvironment to develop more effective therapeutic strategies.

Acknowledgements

This work was supported by Basic and Applied Basic Research Foundation of Guangdong Province (No. 2021B1515140067, 2022A-1515012190), Competitive allocation of special funds for science and technology development in Zhanjiang (No. 2022A01018) and Special Project for Clinical and Basic Sci & Tech Innovation of Guangdong Medical University (GDMULCJC2024117).

Disclosure of conflict of interest

None.

Abbreviations

ESRP1, Epithelial Splicing Regulatory Protein 1; ER, Estrogen Receptor; PR, Progesterone Receptor; BC, Breast Cancer; TNBC, Triple Negative Breast Cancer; SERD, Selective Estrogen Receptor Degrader; CCK-8, Cell Counting Kit-8 assay; EMT, Epithelial-mesenchymal transition; EMT-TF, Epithelial-mesenchymal transition-inducing transcription factors; ECM, Extracellular Matrix; IHC, Immunohistochemistry; OE, Overexpression; RT-qPCR, Reverse Transcription quantitative PCR; WB, Western blot.

Address correspondence to: Yanqin Sun, Department of Pathology, School of Basic Medicine, Guangdong Medical University, No. 2 Wenming East Road, Xiashan District, Zhanjiang 523808, Guangdong, The People's Republic of China. ORCID: 0000-0002-0322-0100; E-mail: sunyanqin@gdmu.edu.cn; Zhi Zhang, Department of Thyroid and Breast Surgery, Dongguan Songshan Lake Central Hospital, Guangdong Medical University, No. 1 Cheung Lung Road, Wong Chau, Shilong Town, Dongguan 523000, Guangdong, The People's Republic of China. E-mail: zhangzhi-0714@gdmu.edu.cn; Dingke Chen, Cancer Center, The Affiliated Dongguan Songshan Lake Central Hospital, Guangdong Medical University, No. 1 Cheung Lung Road, Wong Chau, Shilong Town, Dongguan 523000, Guangdong, The People's Republic of China. E-mail: 714266013@qq.com

References

[1] Sung H, Ferlay J, Siegel RL, Laversanne M, Soerjomataram I, Jemal A and Bray F. Global cancer statistics 2020: GLOBOCAN estimates of incidence and mortality worldwide for 36 cancers in 185 countries. CA Cancer J Clin 2021; 71: 209-249.

[2] Siegel RL, Giaquinto AN and Jemal A. Cancer statistics, 2024. CA Cancer J Clin 2024; 74: 12-49.
[3] Afzal MZ and Vahdat LT. Evolving management of breast cancer in the era of predictive biomarkers and precision medicine. J Pers Med 2024; 14: 719.
[4] Dai Z, Gu XY, Xiang SY, Gong DD, Man CF and Fan Y. Research and application of single-cell sequencing in tumor heterogeneity and drug resistance of circulating tumor cells. Biomark Res 2020; 8: 60.
[5] Gaire RK, Smith L, Humbert P, Bailey J, Stuckey PJ and Haviv I. Discovery and analysis of consistent active sub-networks in cancers. BMC Bioinformatics 2013; 14 Suppl 2: S7.
[6] Hu S, Yin F, Nie L, Wang Y, Qin J and Chen J. Estrogen and estrogen receptor modulators: potential therapeutic strategies for COVID-19 and breast cancer. Front Endocrinol (Lausanne) 2022; 13: 829879.
[7] Hanker AB, Sudhan DR and Arteaga CL. Overcoming endocrine resistance in breast cancer. Cancer Cell 2020; 37: 496-513.
[8] Chen P, Li B and Ou-Yang L. Role of estrogen receptors in health and disease. Front Endocrinol (Lausanne) 2022; 13: 839005.
[9] Hu J, Li G, Zhang P, Zhuang X and Hu G. A CD44v(+) subpopulation of breast cancer stem-like cells with enhanced lung metastasis capacity. Cell Death Dis 2017; 8: e2679.
[10] Lee HH, Lee AJ, Park WS, Lee J, Park J, Park B, Joung JY, Lee KH, Hong D and Kim SH. Epithelial splicing regulatory protein (ESPR1) expression in an unfavorable prognostic factor in prostate cancer patients. Front Oncol 2020; 10: 556650.
[11] Li C, Yin Y, Tao R, Lin Y, Wang T, Shen Q, Li R, Tao K and Liu W. ESRP1-driven alternative splicing of CLSTN1 inhibits the metastasis of gastric cancer. Cell Death Discov 2023; 9: 464.
[12] Ji Y, Ni C, Shen Y, Xu Z, Tang L, Yu F, Zhu L, Lu H, Zhang C, Yang S and Wang X. ESRP1-mediated biogenesis of circPTPN12 inhibits hepatocellular carcinoma progression by PDLIM2/NF-kappaB pathway. Mol Cancer 2024; 23: 143.
[13] Elhasnaoui J, Ferrero G, Miano V, Franchitti L, Tarulli I, Coscujuela Tarrero L, Cutrupi S and De Bortoli M. A regulatory axis between epithelial splicing regulatory proteins and estrogen receptor alpha modulates the alternative transcriptome of luminal breast cancer. Int J Mol Sci 2022; 23: 7835.
[14] Huang Y, Guo J, Han X, Zhao Y, Li X, Xing P, Liu Y, Sun Y, Wu S, Lv X, Zhou L, Zhang Y, Li C, Xie W and Liu Z. Splicing diversity enhances the molecular classification of pituitary neuroendocrine tumors. Nat Commun 2025; 16: 1552.
[15] Gokmen-Polar Y, Neelamraju Y, Goswami CP, Gu Y, Gu X, Nallamothu G, Vieth E, Janga SC, Ryan M and Badve SS. Splicing factor ESRP1 controls ER-positive breast cancer by altering metabolic pathways. EMBO Rep 2019; 20: e46078.
[16] Yang W, Jiang W, Liao W, Yan H, Ai W, Pan Q, Brashear WA, Xu Y, He L and Guo S. An estrogen receptor alpha-derived peptide improves glucose homeostasis during obesity. Nat Commun 2024; 15: 3410.
[17] Du Z, Wang H, Luo S, Yun Z, Wu C, Yang W, Buck M, Zheng W, Hansen AL, Kao HY and Yang S. The sequence-structure-function relationship of intrinsic ERalpha disorder. Nature 2025; 638: 1130-1138.
[18] Qu T, Zhang W, Qi L, Cao L, Liu C, Huang Q, Li G, Li L, Wang Y, Guo Q, Guo Y, Ren D, Gao Y, Wang J, Meng B, Zhang B and Cao W. ISG15 induces ESRP1 to inhibit lung adenocarcinoma progression. Cell Death Dis 2020; 11: 511.
[19] Wang P, Gao X, Zheng W and Zhang J. Potential impact of epithelial splicing regulatory protein 1 (ESRP1) associated with tumor immunity in pancreatic adenocarcinoma. J Proteomics 2024; 308: 105277.
[20] Deng G, Zhou X, Chen L, Yao Y, Li J, Zhang Y, Luo C, Sun L and Tang J. High expression of ESRP1 regulated by circ-0005585 promotes cell colonization in ovarian cancer. Cancer Cell Int 2020; 20: 174.
[21] Chen S, Wu W, Li QH, Xie BM, Shen F, Du YP, Zong ZH, Wang LL, Wei XQ and Zhao Y. Circ-NOLC1 promotes epithelial ovarian cancer tumorigenesis and progression by binding ESRP1 and modulating CDK1 and RhoA expression. Cell Death Discov 2021; 7: 22.
[22] Liu X, Wang Q, Song S, Feng M, Wang X, Li L, Liu Y and Shi C. Epithelial splicing regulatory protein 1 is overexpressed in breast cancer and predicts poor prognosis for breast cancer patients. Med Sci Monit 2021; 27: e931102.
[23] Warzecha CC, Jiang P, Amirikian K, Dittmar KA, Lu H, Shen S, Guo W, Xing Y and Carstens RP. An ESRP-regulated splicing programme is abrogated during the epithelial-mesenchymal transition. EMBO J 2010; 29: 3286-3300.
[24] Warzecha CC, Sato TK, Nabet B, Hogenesch JB and Carstens RP. ESRP1 and ESRP2 are epithelial cell-type-specific regulators of FGFR2 splicing. Mol Cell 2009; 33: 591-601.
[25] Warzecha CC, Shen S, Xing Y and Carstens RP. The epithelial splicing factors ESRP1 and ESRP2 positively and negatively regulate diverse types of alternative splicing events. RNA Biol 2009; 6: 546-562.

[26] Adam-Artigues A, Arenas EJ, Martinez-Sabadell A, Braso-Maristany F, Cervera R, Tormo E, Hernando C, Martinez MT, Carbonell-Asins J, Simon S, Poveda J, Moragon S, Zazo S, Martinez D, Rovira A, Burgues O, Rojo F, Albanell J, Bermejo B, Lluch A, Prat A, Arribas J, Eroles P and Cejalvo JM. Targeting HER2-AXL heterodimerization to overcome resistance to HER2 blockade in breast cancer. Sci Adv 2022; 8: eabk2746.

[27] Mooney SM, Talebian V, Jolly MK, Jia D, Gromala M, Levine H and McConkey BJ. The GRHL2/ZEB feedback loop-a key axis in the regulation of EMT in breast cancer. J Cell Biochem 2017; 118: 2559-2570.

[28] Gokmen-Polar Y, Gu Y, Polar A, Gu X and Badve SS. The role of ESRP1 in the regulation of PHGDH in estrogen receptor-positive breast cancer. Lab Invest 2023; 103: 100002.

[29] Bouris P, Skandalis SS, Piperigkou Z, Afratis N, Karamanou K, Aletras AJ, Moustakas A, Theocharis AD and Karamanos NK. Estrogen receptor alpha mediates epithelial to mesenchymal transition, expression of specific matrix effectors and functional properties of breast cancer cells. Matrix Biol 2015; 43: 42-60.

[30] Cui J, Ren P, Li Y, Ma Y, Wang J, Lin C, Jing L, Tong X, Ma S and Chen J. ESRP1 as a prognostic factor of non-small-cell lung cancer is related to the EMT transcription factor of Twist. Thorac Cancer 2021; 12: 2449-2457.

[31] Horiguchi K, Sakamoto K, Koinuma D, Semba K, Inoue A, Inoue S, Fujii H, Yamaguchi A, Miyazawa K, Miyazono K and Saitoh M. TGF-beta drives epithelial-mesenchymal transition through deltaEF1-mediated downregulation of ESRP. Oncogene 2012; 31: 3190-3201.

[32] Huang Y, Hong W and Wei X. The molecular mechanisms and therapeutic strategies of EMT in tumor progression and metastasis. J Hematol Oncol 2022; 15: 129.

[33] Lee S, Cieply B, Yang Y, Peart N, Glaser C, Chan P and Carstens RP. Esrp1-regulated splicing of arhgef11 isoforms is required for epithelial tight junction integrity. Cell Rep 2018; 25: 2417-2430, e5.

[34] Debnath P, Huirem RS, Dutta P and Palchaudhuri S. Epithelial-mesenchymal transition and its transcription factors. Biosci Rep 2022; 42: BSR20211754.

[35] Papanicolaou M, Parker AL, Yam M, Filipe EC, Wu SZ, Chitty JL, Wyllie K, Tran E, Mok E, Nadalini A, Skhinas JN, Lucas MC, Herrmann D, Nobis M, Pereira BA, Law AMK, Castillo L, Murphy KJ, Zaratzian A, Hastings JF, Croucher DR, Lim E, Oliver BG, Mora FV, Parker BL, Gallego-Ortega D, Swarbrick A, O'Toole S, Timpson P and Cox TR. Temporal profiling of the breast tumour microenvironment reveals collagen XII as a driver of metastasis. Nat Commun 2022; 13: 4587.

[36] Hajimehdipoor H, Tahmasvand Z, Nejad FG, Maresca M and Rajabi S. Rutin promotes proliferation and orchestrates epithelial-mesenchymal transition and angiogenesis in MCF-7 and MDA-MB-231 breast cancer cells. Nutrients 2023; 15: 2884.

[37] Hu H, Ma J, Peng Y, Feng R, Luo C, Zhang M, Tao Z, Chen L, Zhang T, Chen W, Yin Q, Zhai J, Chen J, Yin A, Wang CC and Zhong M. Thrombospondin-1 regulates trophoblast necroptosis via NEDD4-mediated ubiquitination of TAK1 in preeclampsia. Adv Sci (Weinh) 2024; 11: e2309002.

Table S1. Target sequences of siRNAs

Name	Target Sequence (5'-3')
si-ESRP1-#1	GCAGCAAGAUGGAACUUAUTT
si-ESRP1-#2	GCUGCAGUUAUUCCUACAGTT
si-ESRP1-#3	CAGGUGCUGAAUGGAUUCUTT
si-ESRP1-#4	CAACCGAGGAUGGACUUAUTT
siNC	UUCUCCGAACGUGUCACGUTT

Table S2. Primers' sequences

Primer	Sequence (5'-3')
GAPDH-F	CAATGACCCCTTCATTGACC
GAPDH-R	GACAAGCTTCCCGTTCTCAG
ESRP1-F	GAGCACCGAGACCTAGCACTAC
ESRP1-R	GAAACTGGGCTACCTCATTGGAAG
ESR1-F	TGATGA AAGGTGGGATACGA
ESR1-R	AAGGTTGGCAGCTCTCATGT
VIM-F	GGCTCGTCACCTTCGTGA AT
VIM-R	GAGAAATCCTGCTCTCCTCGC
SNAIL1-F	TCAGATGAGGACAGTGGGAAAGG
SNAIL1-R	AAGGAAGAGACTGAAGTAGAGGAGAAG
SLUG-F	AGACCCTGGTTGCTTCAAGGA
SLUG-R	CTCAGATTTGACCTGTCTGCA AA
THBS1-F	ATCCGCAAAGTGACTGAAGAGAAC
THBS1-R	CTGAACTCCGTTGTGATAGCATAGG
CD44-F	ACTGCTTATGAAGGAAACTGGAACC
CD44-R	TGCCTGGATTGTGCTTGTAGAATG
COL4A5-F	GGCTGGCAACTGTAGATGTGTC
COL4A5-R	CGGCTAATTCGTGTCCTCAAGTC
TIMP1-F	CGCTGACATCCGGTTCGT
TIMP1-R	TGTGGAAGTATCCGCAGACACT

Table S3. Correlation between ESRP1 positive and Molecular type of breast cancer

Molecular type	Total	ESRP1 expression		χ^2	P
		Low or negative (%)	High (%)		
Luminal (A+B)	62	19 (30.6)	43 (69.4)	2.703	0.258
Her-2+	13	6 (46.2)	7 (53.8)		
TNBC	23	11 (47.8)	12 (52.2)		